

Computational study on the electrocyclic reactions of [16]annulene†

Ho-Lam Lee and Wai-Kee Li*

Department of Chemistry, The Chinese University of Hong Kong, Shatin, N.T., Hong Kong SAR, China. E-mail: wkli@cuhk.edu.hk; Fax: (852) 2603 5057; Tel: (852) 2609 6281

Received 29th April 2003, Accepted 17th June 2003

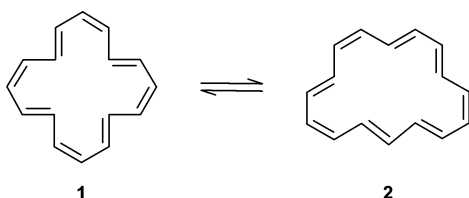
First published as an Advance Article on the web 2nd July 2003

The electrocyclic reactions of [16]annulene have been investigated by *ab initio* and DFT calculations. Among the six conformers of [16]annulene identified, **3**, with C_s symmetry, is taken as the starting reactant for the cyclization reactions of [16]annulene, even though it is 31.4 kJ mol⁻¹ less stable than the most stable conformer, **1**. The pathways of the electrocyclic reactions from reactant **3** to two tricyclic products, **5** and **6**, have been found. All pathways identified are stepwise, *i.e.*, the two ring closure processes occur one after the other. Among the pathways found, the ones with the lowest overall barrier for reactions **3** → **5** and **3** → **6** have the same rate-determining step and hence the same overall barrier, 131.0 kJ mol⁻¹. Thus, based on the barriers calculated, it is not possible to determine whether **5** or **6** is the dominant product in the cyclization reaction of **3**.

Introduction

The pericyclic reactions form one of the major classes of organic reactions. There are three main types of pericyclic processes: electrocyclic reactions, cycloaddition reactions and sigmatropic rearrangements. In the past two decades, the pericyclic reactions of some [*n*]annulenes (*n* = 8, 10, 14, 18) have been studied experimentally and theoretically quite extensively and successfully.^{1–10} These studies revealed unusual differences in these molecules' behaviour in relation to their aromaticity. Rzepa and his group^{7–9} have investigated the Möbius [8]annulenes and their derivatives. Also, they found that some of the pericyclic reactions of [*n*]annulenes (*n* = 10 and 14) proceed *via* a pathway with concerted bond formation, *i.e.*, these molecules exhibit trimorous behaviour.²

Before studying the reactions of [16]annulene, let us first focus on its various conformations. In 1961, [16]annulene was synthesized for the first time.³ However, the conformation of the product was not revealed. Later, Oth and co-workers⁴ prepared **1** by photolysis of the cyclooctatetraene dimer. The structure of **1** was confirmed by X-ray crystallography.⁵ A less stable isomer **2** was suggested to be in equilibrium with **1** in solution.⁶



In the review on annulenes by McNab and co-workers,¹⁰ it was noted that there are at least four stable conformations of [16]annulene and the most stable one was found to be **1**. Later Rzepa² discovered computationally two additional conformations, **3** and **4**, with the latter being a Möbius entity. Very recently, four more new Möbius [16]annulenes have been also found by calculations.¹¹

From the experimental evidence,⁴ a tricyclic species was formed from the heating of **3**, but it was not known whether this reaction was concerted or stepwise. Furthermore, **5**, with

two bridgehead hydrogens pointing in one direction and the remaining two pointing in the opposite direction, was taken as the dominant product by these authors.⁴ If this reaction is stepwise, there are two possible ways for the second step: it can be in the same or in the opposite sense relative to the first. In other words, tricyclic species **6**, with four bridgehead hydrogens pointing in the same direction, is also a possible product. So Rzepa and his group² carried out further investigation on this reaction computationally and they located an electrocyclic transition structure (TS) linking **3** and the bicyclic intermediate **7** at the HF/6-31G level, *i.e.*, the TS for the first step of the aforementioned stepwise reaction. However, they did not locate the TS of either of the two possible second steps of this stepwise reaction. Also, they did not identify the TS for the concerted reaction between reactant **3** and products **5** or **6**. On the other hand, they found that **6** is thermodynamically more stable than **5** and hence they contended that **6**, not **5**, should be the dominant actual product of this reaction.

In the present work, we carried out *ab initio* and density functional theory (DFT) calculations on the concerted as well as stepwise electrocyclic reactions of [16]annulene. It is noted that among the conformers of [16]annulene found, only **3** has the most appropriate conformation to undergo electrocyclic reactions to form the tricyclic product **5** or **6**. So we have chosen **3** as the starting reactant of these reactions. We hope that these computational results will shed some light on the original experimental observations⁴ regarding the electrocyclic reactions of [16]annulene.

Experimental

Methods of calculation

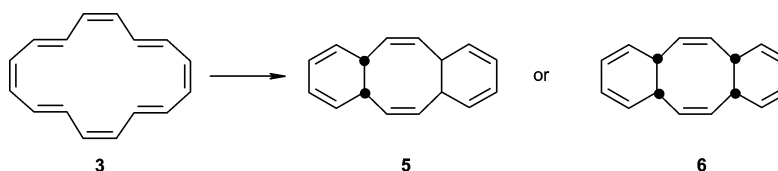
All *ab initio* molecular orbital calculations reported here were carried out using the Gaussian 98 package of programs.¹² The molecular structures for all the species were optimized at the restricted HF/6-31G(d) and B3LYP/6-31G(d) levels.^{13–16} The corresponding HF/6-31G(d) and B3LYP/6-31G(d) harmonic vibrational frequencies, scaled by 0.8929 and 0.9614,¹⁷ respectively, were applied for zero-point vibrational energy (ZPVE) corrections to obtain the total energies at 0 K ($E_0 = E_e + \text{ZPVE}$). In addition to these two theoretical levels, the relative energies for all the species studied have also been calculated at the MP2(Full)/6-31G(d) level, based on the B3LYP/6-31G(d) geometry; these relative energies also include scaled B3LYP/

† Electronic supplementary information (ESI) available: cartesian coordinates of all the equilibrium and transition structures optimized at the B3LYP/6-31G(d) level. See <http://www.rsc.org/suppdata/ob/b3/304654k/>

Table 1 Total energies E_0 , in hartrees, for stationary structures calculated at the restricted HF/6-31G(d), B3LYP/6-31G(d) and MP2(Full)/6-31G(d) levels; relative energies, in kJ mol⁻¹, are given in brackets

Species	HF/6-31G(d) ^a	B3LYP/6-31G(d) ^b	MP2(Full)/6-31G(d) ^c
1	-614.81744 (-34.2)	-618.95557 (-31.5)	-616.91373 (-39.1)
2	-614.81098 (-17.3)	-618.95222 (-22.7)	-616.91329 (-38.0)
3	-614.80440 (0.0)	-618.94359 (0.0)	-616.89882 (0.0)
4	-614.80692 (-6.6)	-618.94507 (-3.9)	-616.90412 (-13.9)
5	-614.81791 (-35.5)	-618.94017 (9.0)	-616.93442 (-93.5)
6	-614.82261 (-47.8)	-618.94352 (0.2)	-616.93680 (-99.7)
7	-614.79435 (26.4)	-618.92510 (48.5)	-616.90508 (-16.4)
8	-614.80071 (9.7)	-618.94083 (7.3)	-616.89927 (-1.2)
9	-614.79488 (25.0)	-618.92737 (42.6)	-616.89247 (16.7)
10	-614.78615 (47.9)	-618.91356 (78.8)	-616.89967 (-2.2)
11	-614.78523 (50.3)	-618.91848 (65.9)	-616.89895 (-0.3)
12	-614.78814 (42.7)	-618.91690 (70.1)	-616.90000 (-3.1)
13	-614.79620 (21.5)	-618.92517 (48.4)	-616.90859 (-25.6)
TSa	-614.73379 (185.4)	-618.89370 (131.0)	-616.86602 (86.1)
TSb	-614.75275 (135.6)	-618.90622 (98.1)	-616.89339 (14.3)
TS^d	-614.68286 (319.1)	-618.86640 (202.7)	-616.84638 (137.7)
TSd	-614.79824 (16.2)	-618.93642 (18.8)	-616.89479 (10.6)
TSe	-614.79256 (31.1)	-618.92594 (46.3)	-616.88971 (23.9)
TSf	-614.72282 (214.2)	-618.88051 (165.6)	-616.85661 (110.8)
TSg	-614.74580 (153.9)	-618.89786 (120.1)	-616.88980 (23.7)
TS^h	-614.72983 (195.8)	-618.89037 (139.7)	-616.86658 (84.7)
TSi	-614.74691 (150.9)	-618.90212 (108.9)	-616.89066 (21.4)
TSj	-614.78623 (47.7)	-618.91667 (70.7)	-616.89951 (-1.8)
TSk	-614.76683 (98.6)	-618.90082 (112.3)	-616.88187 (44.5)
TSⁱ	-614.77937 (65.7)	-618.91239 (81.9)	-616.89312 (15.0)
TS^m	-614.78094 (61.6)	-618.91143 (84.4)	-616.89667 (5.7)

^a Including ZPVE (scaled by 0.8929). ^b Including ZPVE (scaled by 0.9614). ^c Single-point energies calculated using B3LYP/6-31G(d) geometries; including B3LYP/6-31G(d) ZPVE (scaled by 0.9614). ^d **TS^d** has two imaginary vibrational frequencies at both levels and hence is not a true TS. See text for details.



6-31G(d) ZPVEs. In this paper, we use the notation **1**, **2**, ..., etc. to label the stable species found. All these structures have only real vibrational frequencies. Additionally, many TSs of reactions have been identified and they are denoted as **TSa**, **TSb**, ..., etc. For each TS found, its "reactants" and "products" were confirmed by intrinsic reaction coordinate (IRC)^{18,19} calculations.

Results and discussion

Table 1 lists the total energies E_0 and relative energies ΔE for all the stationary structures calculated in this work. Fig. 1 shows the structures of all the stable species studied in this work, while the structures of all the TSs located are displayed in Fig. 2. Among the 13 stable species displayed in Fig. 1, **1**–**4**, **8** and **9** represent conformers of [16]annulene, **7** and **10**–**13** are bicyclic intermediates for the electrocyclic reactions of **3**, while **5** and **6** are the tricyclic products of these reactions. Figs. 3 and 4 show the schematic B3LYP/6-31G(d) potential energy surfaces (PESs) for reactions **3** \rightarrow **6** and **3** \rightarrow **5**, respectively. In the courses of these two reactions, bicyclic intermediates **7**, **10** and **11** have been identified. The schematic reaction pathways linking bicyclic intermediates **7** and **10** are shown in Fig. 5. Since the structure of **11** is very different from those of **7** and **10**, we did not attempt to find the pathway linking **11** with **7** or **10**. Finally, Fig. 6 integrates the pathways shown in Figs. 3–5 for easy comparison. In Figs. 3–6, **3** is the reference species for all the relative energies. In the figures, the structures of the species are not drawn to scale, while the exact structure may be obtained by making use of the ESI†. In the following discussion, all the

relative energies mentioned refer to the results calculated at the B3LYP/6-31G(d) level at 0 K, unless otherwise mentioned.

Reaction (1): **3** \rightarrow **6**

From Fig. 1, it is seen that **3** is one of the conformations of [16]annulene. At the HF/6-31G(d) level, **3** has C_{2v} symmetry with four internal hydrogens pointing upwards. At the B3LYP/6-31G(d) level, the symmetry changes to C_s and the four internal hydrogens point less upwards and nearly lie on the skeletal plane. Energetically, **3** is 31.4 kJ mol⁻¹ less stable than the most stable conformation found, **1**. We failed to locate any pathway connecting **1** and **3**, but, according to Oth and co-workers,⁴ **1** has "great conformational mobility" and equilibration of **1** and **3** is "immediately understandable." In this section we confine our attention to the reaction **3** \rightarrow **6**.

As shown in Fig. 3, **3** first undergoes ring closure to form intermediate **7** via **TSa** and this TS was first located by Rzepa and co-workers.² In the present study, we have found an additional TS, **TSb**, which connects **7** and the expected product, **6**. Structurally, **6** has C_2 symmetry and its four internal hydrogens point in the same direction, upwards. The overall energy barrier for this reaction is 131.0 kJ mol⁻¹, which is the relative energy of **TSa**.

We also attempted to locate the concerted TS for this reaction, i.e., the TS for the one-step pathway of **3** \rightarrow (TS) \rightarrow **6**. A trimerous² stationary point, called **TS^c**, apparently corresponding to this concerted step has been located. However, **TS^c** was found to have two imaginary frequencies of nearly equal magnitude, 525i and 500i cm⁻¹. Hence **TS^c** is not a true TS. The transition vector with the smaller negative force

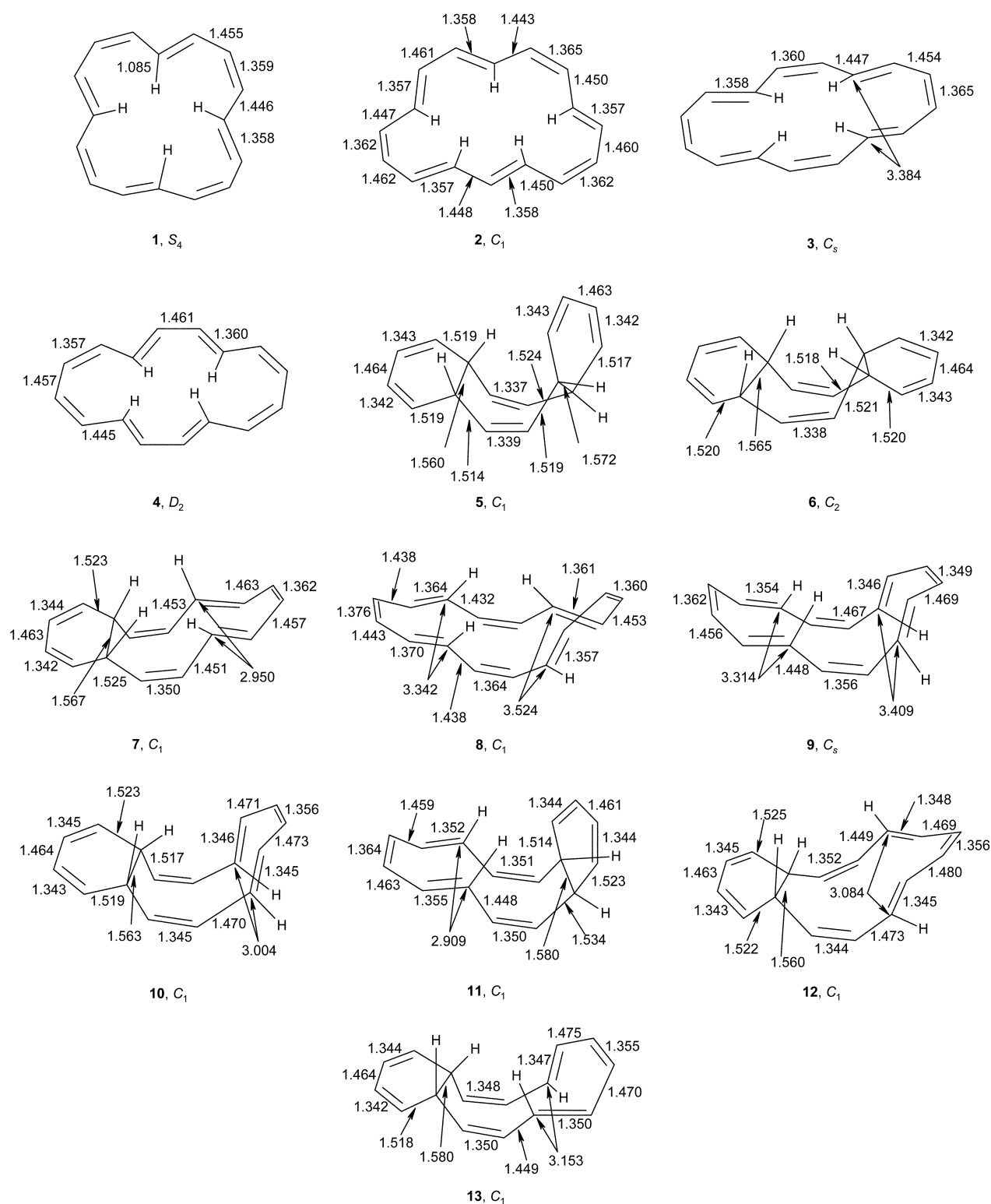


Fig. 1 The structures of the stable species studied in this work optimized at the B3LYP/6-31G(d) level. All bond lengths are in ångströms.

constant (with $\nu = 500i\text{ cm}^{-1}$) is similar to that for **TSa**, which leads to the formation of *one* C–C bond. On the other hand, the remaining transition vector (with $\nu = 525i\text{ cm}^{-1}$) of **TSc** corresponds to the concomitant formation of *two* C–C bonds. However, repeated effort to eliminate the imaginary vibrational frequency with $\nu = 500i\text{ cm}^{-1}$ failed. In other words, we also failed to locate the concerted TS for $3 \rightarrow 6$. It is of interest to note that **TSc** is about 72 kJ mol^{-1} less stable than **TSa**. Hence, if the one-step TS for $3 \rightarrow 6$ exists, it is still likely to be less stable than **TSa**. In other words, reaction $3 \rightarrow 6$ is likely to be stepwise.

Reaction (2): $3 \rightarrow 5$

From Fig. 4, we see that the pathway of this reaction is more complicated than that of reaction (1). In the initial step, one of the C=C bonds of **3** flips upwards to form **8** via **TSd**, with a relatively smaller energy cost of 18.8 kJ mol^{-1} . In **8**, three of the four internal hydrogens point upwards, while the remaining one points downwards. Flipping of the “opposite” C=C bond in **8** will lead to the formation of **9** via **TSe**. Note that **8** and **9** are two of the (six) aforementioned stable conformations of [16]annulene. It is worth noting here that **3** has all four internal

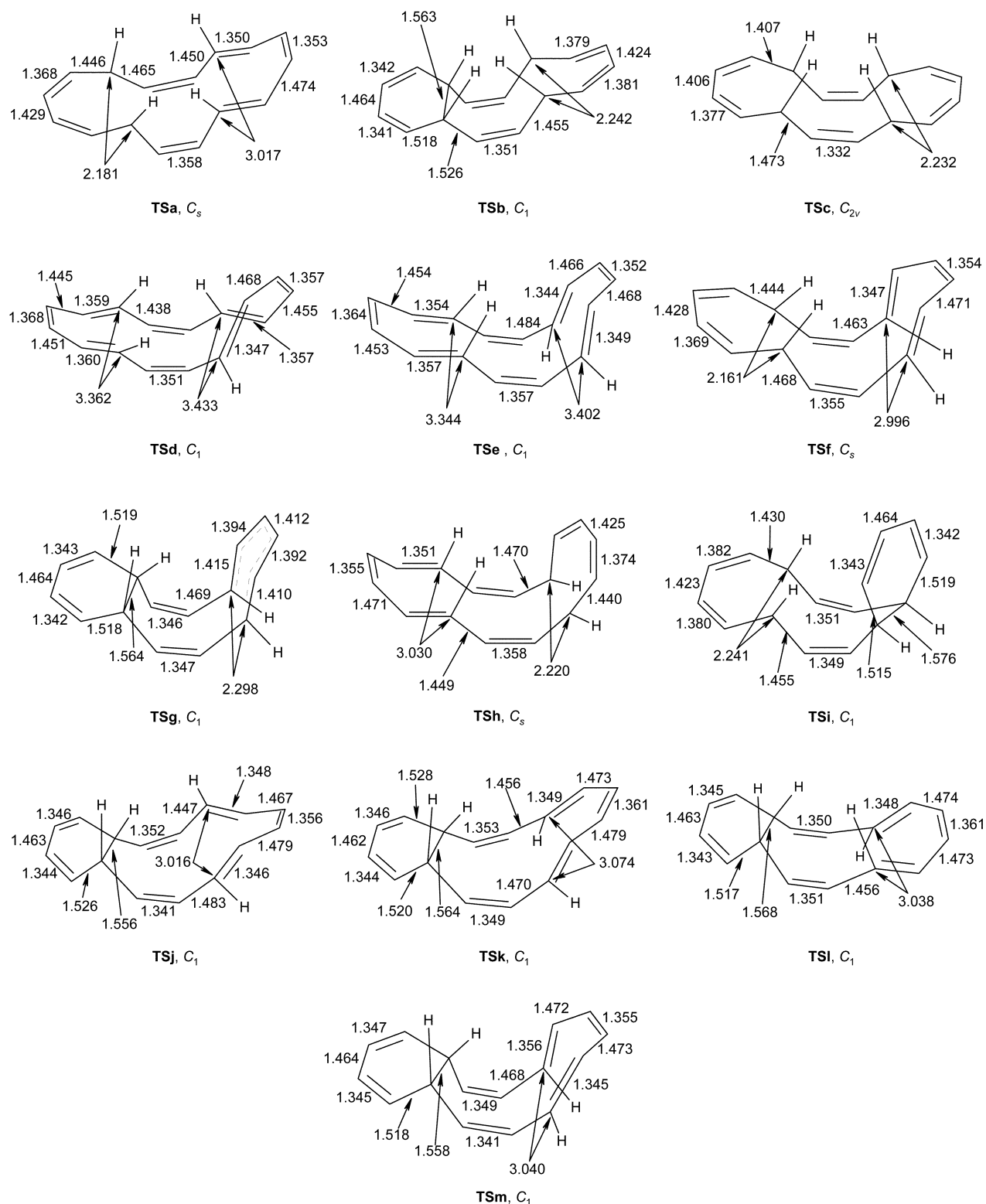


Fig. 2 The structures of the transition structures studied in this work optimized at the B3LYP/6-31G(d) level. All bond lengths are in Å.

hydrogens pointing in the same directions. On the other hand, in **9**, two hydrogens point to one side and the other two point to the opposite side. Also, **8** and **9** have C_1 and C_s symmetry, respectively. Energetically, **9** is 35.3 kJ mol⁻¹ less stable than **8** and the overall energy barrier for the two-step reaction **3** → **9** is 46.3 kJ mol⁻¹. Among **3**, **8** and **9**, only **9** has the appropriate conformation to undergo electrocyclic reactions to form the tricyclic product **5**. There are two ways for **9** to be transformed into **5**, denoted as pathways 2A and 2B. In pathway 2A, **9** first undergoes a ring closure to form a bicyclic intermediate **10** via **TSf**. This is the rate-determining step of pathway 2A.

Subsequently **10** undergoes another ring closure to yield the tricyclic product **5** via **TSg**. The overall energy barrier for this pathway is 165.6 kJ mol⁻¹. On the other hand, in pathway 2B, the ring closure on **9** takes place in the reverse order. Since **5** has C_1 symmetry, the two six-membered carbon rings are not equivalent. In pathway 2B, **9** undergoes ring closure via **TSh** to form bicyclic intermediate **11**, which undergoes yet another ring closure reaction via **TSi** to yield tricyclic product **5**. Intermediate **11** of pathway 2B is more stable than the corresponding intermediate **10** in pathway 2A. Also, **TSh** and **TSi** of pathway 2B are more stable than the corresponding transition structures

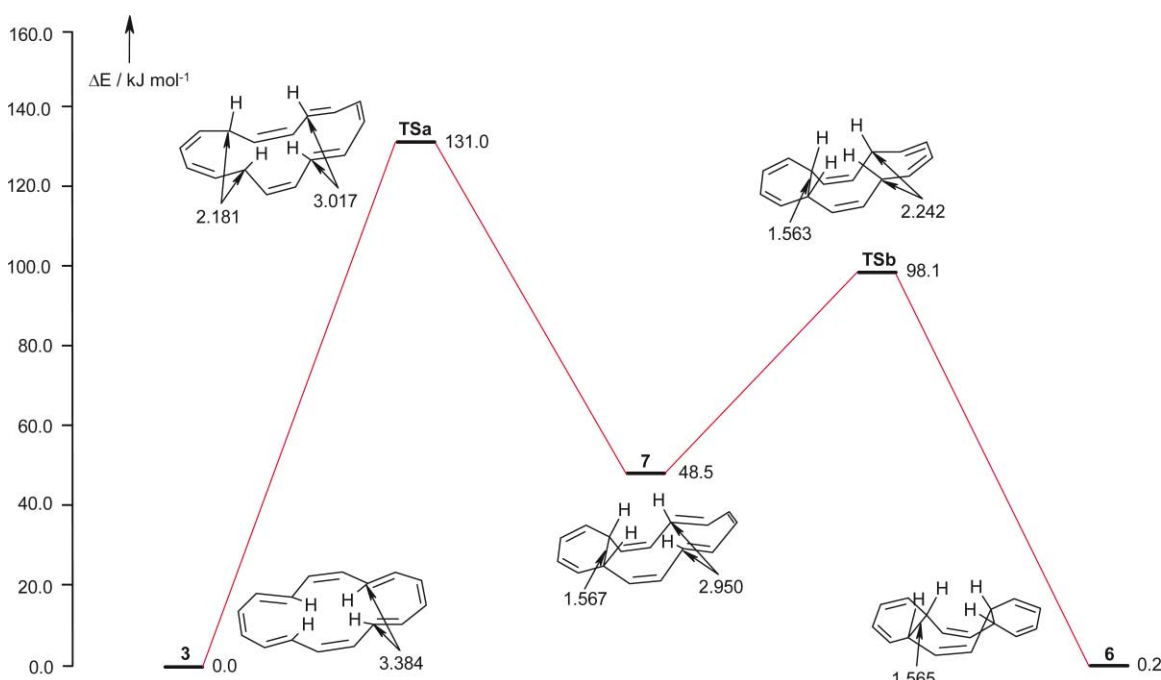


Fig. 3 Potential energy surface showing the possible mechanism for reaction (1), $3 \rightarrow 6$, calculated at the B3LYP/6-31G(d) level.

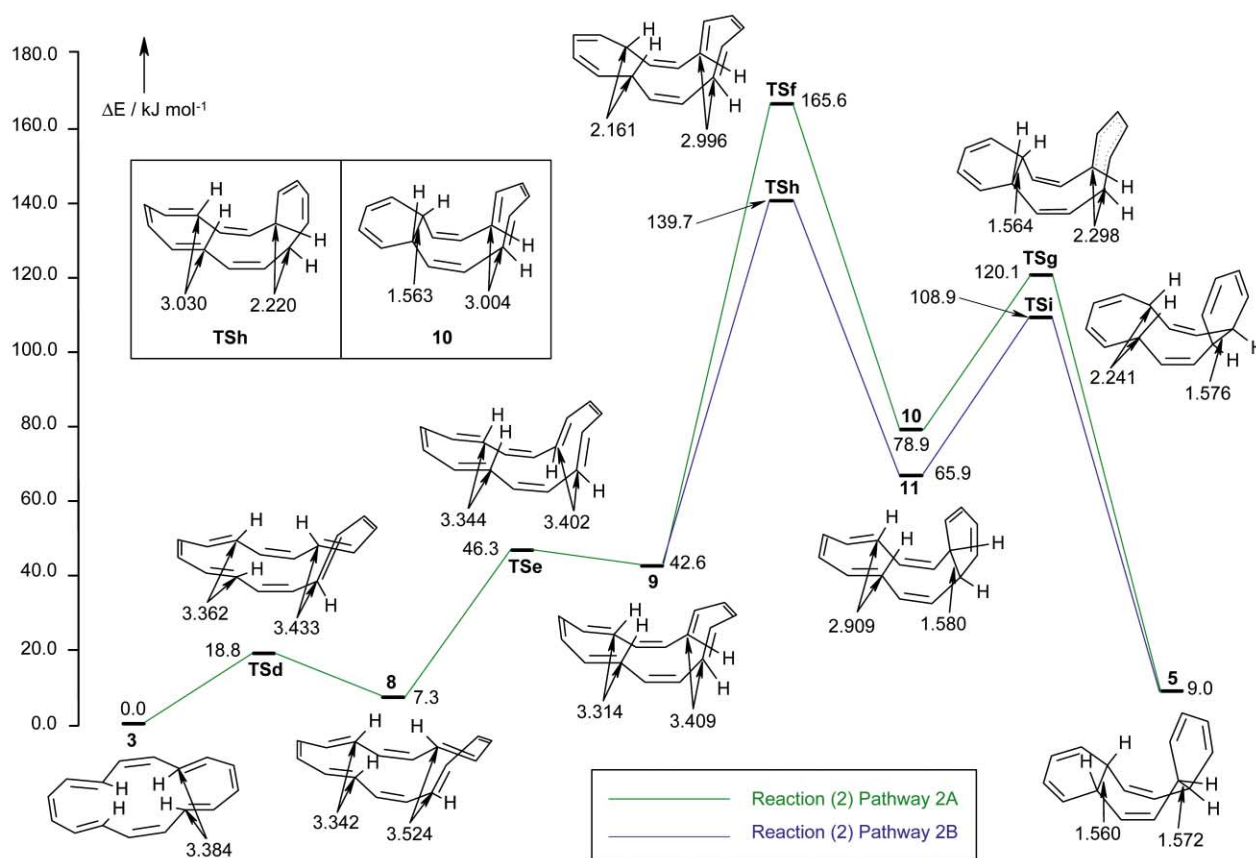


Fig. 4 Potential energy surface showing the possible mechanisms for reaction (2), $3 \rightarrow 5$, calculated at the B3LYP/6-31G(d) level.

TSf and TSg of pathway 2A. The overall energy barrier for pathway 2B is about 26 kJ mol^{-1} lower than that for pathway 2A, so pathway 2B is more energetically favourable.

Comparing reactions (1) and (2), product **6** of reaction (1) has all four internal hydrogens pointing in the same direction, while product **5** of reaction (2) has two hydrogens pointing in one direction and the remaining two pointing in the opposite direction. Considering only the three pathways for reactions (1) and (2) discussed so far, it may be concluded that, since the barrier for reaction (1) is about 9 kJ mol^{-1} less than that of

reaction (2), the (slightly) dominant product observed in the experiments of Oth and co-workers⁴ should be **6**. This conclusion is not shared by the experimentalists, who, by considering qualitatively the steric congestion among the four internal hydrogens in **6**, preferred **5** to be the major product. However, as seen from Table 1, **6** is actually thermodynamically more stable than **5** by about 9 kJ mol^{-1} ; this result was also obtained by Rzepa and co-workers.²

Finally, it is mentioned that we also failed to locate the concerted TS for reaction (2). More importantly, we note that the

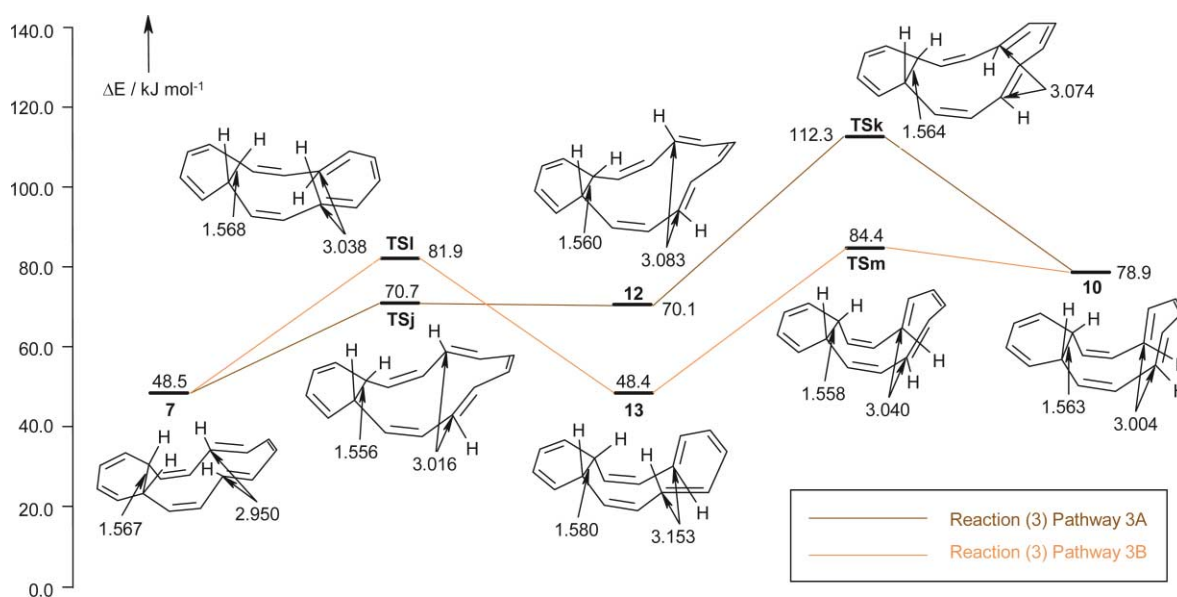


Fig. 5 Potential energy surface showing the possible mechanisms for reaction (3), $7 \rightarrow 10$, calculated at the B3LYP/6-31G(d) level.

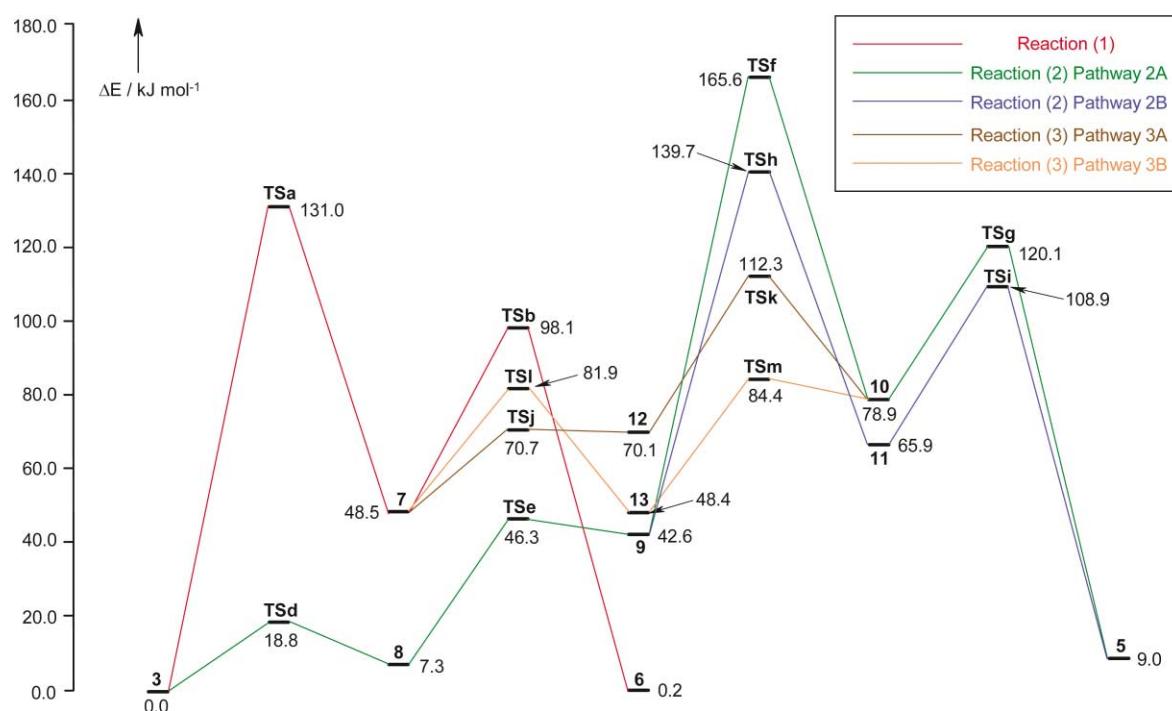


Fig. 6 Energy profiles of reactions (1) to (3) calculated at the B3LYP/6-31G(d) level.

pathway suggested in this section is just one of the possible pathways for the transformation from **3** to **5**. In the following, we will propose alternative pathways for this reaction.

Reaction (3): $7 \rightarrow 10$

In our previous discussion, we discovered two bicyclic intermediates **7** and **10** in reactions (1) and (2), respectively. In bicyclic species **7** and **10**, both with C_1 symmetry, the six-membered rings of **7** and **10** are similar to each other, with two internal hydrogens pointing upwards. Also, the internal hydrogens in **7** have the “four-up” conformation, while those in **10** have the “two-up-two-down” conformation. In this section, we study the reaction pathways linking these two intermediates. By connecting **7** and **10**, the paths for the cyclization reactions of **3** would become much more complicated. As can be seen from Fig. 5, there are two ways, denoted as pathways 3A and 3B, via which **7** and **10** can transform into one another.

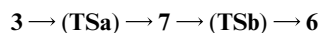
In pathway 3A, **7** first flips one of its internal hydrogens on

the twelve-membered ring downwards to form intermediate **12** via **TSj**. In other words, **12** has the “three-up-one-down” conformation. Subsequently, the other internal hydrogen on the twelve-membered ring also flips downwards to form **10** via **TSk**. The overall barrier for pathway 3A is about 64 kJ mol^{-1} . On the other hand, in pathway 3B, the flipping of the internal hydrogens on the twelve-membered ring takes place in the reverse order. Since **7** has C_1 symmetry, the two internal hydrogens on the twelve-membered ring are not equivalent. In pathway 3B, the intermediate with the “three-up-one-down” conformation is called **13**, which is more stable than the corresponding intermediate **12** in pathway 3A. The overall barrier for pathway 3B is about 46 kJ mol^{-1} , which is 18 kJ mol^{-1} lower than that for pathway 3A.

We have also attempted to locate the concerted TS for $7 \rightarrow 10$. In the course of our search, we found that the twelve-membered ring is not large enough to accommodate the concomitant flipping of its two internal hydrogens. Hence this TS is unlikely to exist.

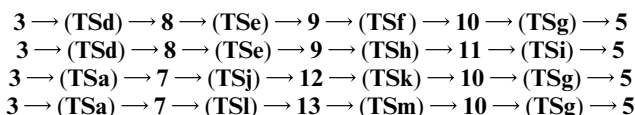
Overall reaction: $3 \rightarrow 5$ and/or 6 ?

All the results discussed so far are summarized in Fig. 6. We can see that there is only one pathway for reaction $3 \rightarrow 6$:



This is the pathway depicted in Fig. 3. As mentioned earlier, the rate-determining step is the formation of intermediate **7** from reactant **3**, and the overall barrier is $131.0 \text{ kJ mol}^{-1}$.

On the other hand, there are four possible pathways for reaction $3 \rightarrow 5$:



The overall barriers for these four pathways are 165.6, 139.7, 131.0 and $131.0 \text{ kJ mol}^{-1}$, respectively, if we consider only the largest barrier of the elementary processes. In other words, the last two pathways have the same overall barrier, which is the same barrier for $3 \rightarrow 6$.

Before we compare the calculated results at different levels with the experimental data,⁴ we find that the theoretical results are not in good agreement. The calculated exothermicities at the HF/6-31G(d) and MP2(Full)/6-31G(d) levels are -14 and -60 kJ mol^{-1} , respectively, while, at the B3LYP/6-31G(d) level, the reaction is *endothermic* by about 30 kJ mol^{-1} . Experimentally, the reaction enthalpy of the cyclization of **1** was *estimated* to be -38 kJ mol^{-1} at 20°C in a variety of solvents including benzene, ether, acetone and CS_2 . In other words, the B3LYP/6-31G(d) method may not be very appropriate for the extensively conjugated systems such as **5** and **6**. However, all three theoretical levels employed show the same trend for the overall energy profile of the reactions. In addition, the calculated overall energy barriers at the MP2(Full)/6-31G(d) and B3LYP/6-31G(d) levels are in qualitative agreement with the estimated experimental result. Experimentally, under the aforementioned condition, the barrier was *estimated* to be 92 kJ mol^{-1} .⁴ At the HF/6-31G(d), B3LYP/6-31G(d) and MP2(Full)/6-31G(d) levels of theory, this quantity is calculated to be 220, 162 and 125 kJ mol^{-1} , respectively.

To sum up, for the electrocyclic reactions of [16]annulene, based on the barriers calculated by *ab initio* and DFT methods, it is not possible to determine whether products **5** or **6** would dominate. On the other hand, we agree with Rzepa and co-workers that, thermodynamically, **6** is the preferred product.

Conclusion

Ab initio and DFT methods have been employed to study the electrocyclic reactions of [16]annulene. Conformer **3**, with C_s symmetry and the proper orientation for the internal hydrogens, is taken as the starting reactant for the cyclization reaction of [16]annulene, even though it is 31.4 kJ mol^{-1} less stable than the most stable conformer found, **1**. The pathways of the electrocyclic reactions from reactant **3** to two expected tricyclic products, **5** and **6**, have been found. All pathways identified are stepwise, *i.e.*, the two ring closure reactions take place one at a time. Among the pathways found, the ones with the lowest overall barrier for reactions $3 \rightarrow 5$ and $3 \rightarrow 6$ have the same rate-determining step and hence the same overall barrier, $131.0 \text{ kJ mol}^{-1}$. Thus, based on the barriers calculated, it is not

possible to determine which is the dominant product in this reaction.

Furthermore, two new conformations of [16]annulene, **8** and **9**, have been found and they are less stable than **3** by 7.3 and 42.6 kJ mol^{-1} , respectively. In the course of studying the electrocyclic reactions of **3**, the TSs connecting conformers **3**, **8** and **9** of [16]annulene were also located. Finally, we also identified a trimerous stationary point, **TSc**, apparently corresponding to a concerted pathway for the reaction of $3 \rightarrow 6$. However, **TSc** has two imaginary vibrational frequencies, which means it is not a true TS. Indeed, all of our attempts to locate the TSs of the concerted pathways of all the reactions studied here failed. So the electrocyclic reactions of [16]annulene are likely to be stepwise.

Acknowledgements

The authors are grateful to the Computer Services Centre of The Chinese University of Hong Kong for its allocation of computer time on the SGI Origin 2000 High-Performance Server. The work described in this paper was supported by a grant from the Research Grants Council of the Hong Kong Special Administrative Region (Project No. CUHK4275/00P).

References

- 1 C. Conesa and H. S. Rzepa, *J. Chem. Soc., Perkin Trans. 2*, 1998, 2695.
- 2 S. Martin-Santamaria, B. Lavan and H. S. Rzepa, *J. Chem. Soc., Perkin Trans. 2*, 2000, 1415.
- 3 F. Sondheimer and Y. Gaoni, *J. Am. Chem. Soc.*, 1961, **83**, 4883.
- 4 G. Schröder, W. Martin and J. F. M. Oth, *Angew. Chem., Int. Ed. Engl.*, 1967, **6**, 870.
- 5 S. M. Johnson, I. C. Paul and G. S. B. King, *J. Chem. Soc. B*, 1970, 643.
- 6 J. F. M. Oth and J.-M. Gilles, *Tetrahedron Lett.*, 1968, 6259.
- 7 S. Martin-Santamaria, B. Lavan and H. S. Rzepa, *J. Chem. Soc., Perkin Trans. 2*, 2000, 2372.
- 8 W. L. Karney, C. J. Kastrop, S. P. Oldfield and H. S. Rzepa, *J. Chem. Soc., Perkin Trans. 2*, 2002, 388.
- 9 C. J. Kastrop, S. P. Oldfield and H. S. Rzepa, *Chem. Commun.*, 2002, 642.
- 10 R. D. Kennedy, D. Lloyd and H. McNab, *J. Chem. Soc., Perkin Trans. 1*, 2002, 1601.
- 11 C. Castro, C. M. Isborn, W. L. Karney, M. Mauksch and P. v. R. Schleyer, *Org. Lett.*, 2002, **4**, 3431.
- 12 M. J. Frisch, G. W. Trucks, H. B. Schlegel, G. E. Scuseria, M. A. Robb, J. R. Cheeseman, V. G. Zakrzewski, J. A. Montgomery, R. E. Stratmann, J. C. Burant, S. Dapprich, J. M. Millam, A. D. Daniels, K. N. Kudin, M. C. Strain, O. Farkas, J. Tomasi, V. Barone, M. Cossi, R. Cammi, B. Mennucci, C. Pomelli, C. Adamo, S. Clifford, J. Ochterski, G. A. Petersson, P. Y. Ayala, Q. Cui, K. Morokuma, D. K. Malick, A. D. Rabuck, K. Raghavachari, J. B. Foresman, J. Cioslowski, J. V. Ortiz, B. B. Stefanov, G. Liu, A. Liashenko, P. Piskorz, P. I. Komaromi, R. Gomperts, R. L. Martin, D. J. Fox, T. Keith, M. A. Al-Laham, C. Y. Peng, A. Nanayakkara, C. Gonzalez, M. Challacombe, P. M. W. Gill, B. G. Johnson, W. Chen, M. W. Wong, J. L. Andres, M. Head-Gordon, E. S. Replogle and J. A. Pople, *Gaussian 98*, Revision A.9, Gaussian, Inc., Pittsburgh, PA, 1998.
- 13 A. D. Becke, *J. Chem. Phys.*, 1993, **98**, 5648.
- 14 C. Lee, W. Yang and R. G. Parr, *Phys. Rev. B*, 1988, **37**, 785.
- 15 P. J. Stephens, F. J. Devlin, C. F. Chabalowski and M. J. Frisch, *J. Phys. Chem.*, 1994, **98**, 11623.
- 16 K. L. Bak, F. J. Devlin, C. S. Ashvar, P. R. Taylor, M. J. Frisch and P. J. Stephens, *J. Phys. Chem.*, 1995, **99**, 14918.
- 17 A. P. Scott and L. Radom, *J. Phys. Chem.*, 1996, **100**, 16502.
- 18 C. Gonzalez and H. B. Schlegel, *J. Chem. Phys.*, 1989, **90**, 2154.
- 19 C. Gonzalez and H. B. Schlegel, *J. Chem. Phys.*, 1990, **94**, 5523.